

Thermodynamic Evaluation of the system Ta–O and Preliminary Assessment of the Systems Al–Nb–O and Al–Ta–O

Julian Gebauer,* Peter Franke, and Hans Jürgen Seifert

The binary tantalum–oxygen system is assessed using the CALculation of PHase Diagrams (CALPHAD) method with experimental data from the literature. The oxygen solubility in the Ta solid-solution phase is discussed and modeled. The low- and high-temperature modifications of Ta₂O₅ are described as stoichiometric compounds. This dataset is extended into the ternary Al–Ta–O system by complementing it with binary datasets for Al–O and Al–Ta from the literature and adding mixed-oxide AlTaO₄. The dataset for the ternary system Al–Nb–O is created by combining the three corresponding binary datasets from the literature and by assessing the quasibinary section Al₂O₃–Nb₂O₅. The ternary aluminum niobates are described as stoichiometric compounds. Phase equilibria between refractory metals and alumina at high temperature are discussed.

scanning calorimetry (DSC), differential thermal analysis (DTA), X-Ray diffraction (XRD), and drop-solution calorimetry experiments for the ternary systems are planned for the near future and will then lead to reassessments of the datasets.

The CALculation of PHase Diagrams (CALPHAD) method is used to consolidate information about the coupling of thermochemical data and phase diagrams in a database. In a CALPHAD database, mathematical models are used to describe the Gibbs energy functions for all phases occurring in the system of interest. Those functions can be used for the calculation of several thermodynamic and thermophysical properties like enthalpy,

entropy, specific heat, and phase diagrams. A general description for Gibbs energy is given in Equation (1).^[1] This model contains reference, ideal mixing, and excess terms (Equation (2)–(4)).^[1] The widely used sublattice model is expressed in compound energy formalism (CEF). The constituents of crystalline phases generally prefer to occupy different lattice sites. Therefore, sublattice models are used to describe the mixing enthalpies and mixing entropies of these phases. In the framework of the CEF, the Gibbs energy of these phases is given by the following set of equations.^[1,2]

$$G^\varphi = \text{ref}G^\varphi + \text{id}G^\varphi + \text{ex}G^\varphi \quad (1)$$

$$\text{ref}G^\varphi = \sum_i \sum_j \cdots \sum_k Y_i^{(1)} Y_j^{(2)} \cdots Y_k^{(s)} G_{i:j:\dots:k}^\varphi \quad (2)$$

$$\text{id}G^\varphi = \frac{1}{\sum_s n^{(s)}} RT \sum_s \sum_i n^{(s)} Y_i^{(s)} \ln Y_i^{(s)} \quad (3)$$

$$\text{ex}G^\varphi = \text{ex}^2G^\varphi + \text{ex}^3G^\varphi + \dots = \sum_s \sum_i \sum_j Y_i^{(s)} Y_j^{(s)} \sum_{r \neq s} Y_k^{(r)} L_{i:j:\dots:k}^\varphi(T) + \dots + \text{ex}^3G^\varphi + \dots \quad (4)$$

The mole fraction of the species i in the sublattice s is denoted as site fraction $Y_i^{(s)}$. Binary (ex^2G^φ) and ternary (ex^3G^φ) excess terms correspond to the binary and ternary interactions in the sublattices.

For the description of molten oxides, the ionic two-sublattice model introduced by Hillert et al.^[3] can be used. In this model, cations (C) are distributed on one sublattice and anions (A),

1. Introduction

Refractory metal–alumina composites are of interest for new materials for high-temperature applications. The targeted synergy effects of the composites compared with pure materials are higher oxidation resistance and better thermal shock stability. Knowledge about phase transformations, reactions during the sintering process, and long-term heat treatments are a fundamental basis in developing such new materials. In the present work, thermodynamic datasets are developed for the binary system Ta–O and for the two ternary systems Al–Nb–O and Al–Ta–O. The binary Ta–O system is newly assessed to better represent the equilibria with the liquid. The remaining binary datasets are available in sufficient quality in the literature. The ternary datasets will be in preliminary status because differential

J. Gebauer, P. Franke, H. J. Seifert
Institute for Applied Materials - Applied Materials Physics
Karlsruhe Institute of Technology
Hermann-von-Helmholtz Platz 1, 76344 Eggenstein-Leopoldshafen,
Germany
E-mail: julian.gebauer@kit.edu

 The ORCID identification number(s) for the author(s) of this article can be found under <https://doi.org/10.1002/adem.202200162>.

© 2022 The Authors. Advanced Engineering Materials published by Wiley-VCH GmbH. This is an open access article under the terms of the Creative Commons Attribution-NonCommercial-NoDerivs License, which permits use and distribution in any medium, provided the original work is properly cited, the use is non-commercial and no modifications or adaptations are made.

DOI: 10.1002/adem.202200162

neutral species (B), and vacancies (Va) on the second sublattice^[2]

$$(C_i^{v_i+})_P(A_j^{v_j-}, Va, B_k^0)_Q \quad (5)$$

The charge of anions and cations is described by v_i and the indices i and j and k refer to the constituents. P and Q are the number of sites on the two sublattices, which are not constant to maintain the electroneutrality.

With this model, a liquid that changes its character from metallic to ionic over the composition range can be described.^[3] To apply this model to a metallic system, the first sublattice is filled corresponding cations while the second sublattice is filled with negatively charged vacancies. Then the ionic liquid model can represent the interaction modeled in the original metallic system.^[4]

For all calculations, plots, and optimization steps, ThermoCalc software^[5] was used.

2. Evaluation of Literature Data

For ternary systems, no CALPHAD modeling is found in the literature. For the binary systems, CALPHAD-type datasets from the literature are selected according to their mutual compatibility.

2.1. Al–O

Two datasets were published: one by Hallstedt^[6] and the other by Taylor et al.^[7]

The one of Hallstedt is set up with an ionic liquid model containing the neutral species $AlO_{3/2}$. In contrast, the model of Taylor et al. only uses the ions Al^{3+} and O^{2-} and vacancies, to describe the ionic liquid. From each parameter set, the same phase diagram can be calculated. Both have the equilibria with the gas phase implemented.

2.2. Nb–O

A thermodynamic evaluation of the system Nb–O was published by Massih and Jerlerud Pérez,^[8] which was based on an unpublished evaluation of this system by Dupin and Ansara.^[9] In both datasets, the ionic liquid is modeled with neutral species NbO_2 and $NbO_{5/2}$, together with the ions Nb^{2+} and O^{2-} and vacancies. The two other oxidation states of niobium, Nb^{4+} and Nb^{5+} , are not used. Massih and Jerlerud Pérez^[8] have reviewed several experimental data from the literature and provided a reliable parameter set to fit those data very well.

2.3. Al–Nb

The datasets of Zhu et al.^[10] and Witusiewicz et al.^[11] have been reviewed for this work. Witusiewicz et al.^[11] mainly revised the parameters for the solid–liquid equilibria and considered experimental data that was published after the assessment of Zhu et al.^[10] He et al.^[12] presented a revision of the work of Witusiewicz et al.^[11] with the background of the Al–Nb system being extrapolated to the ternary system with cobalt. Within their work, problems with the ternary solid solution of Nb_2Al

occurred. When substituting cobalt into the sublattices of the Nb_2Al model, the homogeneity range extended too strongly to the niobium rich side, forcing the authors to reevaluate the binary system. He et al.^[12] used the same experimental data as Witusiewicz et al.^[11] used. As no oxygen solubility in Nb_2Al is considered in the work of He et al.^[12] and is not modeled in the present work, the parameter set of the work of Witusiewicz et al.^[11] is accepted for this work.

2.4. Al–Ta

Du and Schmid-Fetzer^[13] published a dataset for the Al–Ta system, which was later revised by Witusiewicz et al.^[14] Considering experimental data from the literature and their own experiments Witusiewicz et al.^[14] provided a parameter set that is accepted for this work.

2.5. Ta–O

The thermodynamic dataset for Ta–O is assessed in the present work. However, very recently, another evaluation of this system was published by Meisner et al.^[15] Their work is discussed in Section 4.1 and both investigations are compared.

3. Thermodynamic Modeling

3.1. Ta–O

An overview of the thermodynamics and the phase diagram of the Ta–O system was given by Garg et al.^[16] The stable phases of this system are metallic Ta, dissolving up to 5.7 at% oxygen, stoichiometric tantalum oxide, which exists in two modifications: tetragonal α - Ta_2O_5 and orthorhombic β - Ta_2O_5 , and the liquid phase, which has a miscibility gap with a monotectic reaction. Apart from the stable phases mentioned here, a large number of metastable phases in the Ta–O system have been reported in the literature, which are compiled in the review by Garg et al.^[16]

The phase diagram in its original form was established by Jehn and Olzi.^[17] However, the locations of the liquidus lines are still subject to great uncertainty, especially in the Ta-rich region and for the miscibility gap. The oxygen solubility in Ta found by Jehn and Olzi^[17] has been confirmed by several studies.^[18–21]

Thermodynamic data on the Ta–O system are available in the literature for the gaseous species TaO and TaO_2 , as well as for solid Ta_2O_5 in both modifications α - Ta_2O_5 and β - Ta_2O_5 . The published thermodynamic data of these oxides have been critically reviewed and supplemented by new experimental investigations by Jacob et al.^[22] An improved dataset for Ta_2O_5 in the range from room temperature to 2200 K was created, which contains heat capacity, entropy, enthalpy, and the standard Gibbs energies of formation of Ta_2O_5 for the two solid oxides and the melt.

The Gibbs energies for the formation of Ta_2O_5 were measured in an electrochemical solid-state cell.^[22] A mixture of Ta_2O_5 and Ta powder was used as the working electrode and a mixture of MnO with Mn powder as the reference electrode. ThO_2 stabilized with Y_2O_3 served as the electrolyte. When calculating the

standard Gibbs energy of formation, the influence of the oxygen solubility in metallic Ta on the activity of Ta is also taken into account by Jacob et al.^[22] Comparing these values for the standard Gibbs energy of formation of Ta₂O₅, Jacob et al.^[22] found the best agreement with the data of Ignatowicz and Davies^[23] and Rezukhina and Kravchenko.^[24] The corresponding values from the JANAF tables,^[25] on the other hand, are from 2.5 (at 1027 °C) to 5 kJ mol⁻¹ (at 727 °C) below the values from Jacob et al.^[22]

Jacob et al.^[22] provide the data of their assessment in a table, which lists at regular temperature intervals the heat capacities (*c_p*), entropies, enthalpies of formation, and Gibbs energies of formation of the oxides. In addition, Mayer–Kelly-type equations are given for the heat capacity, the entropy, and the enthalpy of the oxides. These data are the basic inputs for the determination of the Gibbs energy functions of the oxides in the database of the present work. While the coefficients of the *c_p* functions were adopted unchanged from the study by Jacob et al.,^[22] it was necessary to adjust the enthalpy and entropy increments of the Gibbs energy functions for the oxides to obtain compatibility with the SGTE recommendations for the data of the elements.^[26] Due to these adjustments, the standard Gibbs energy of formation and the standard enthalpy of formation of β-Ta₂O₅ at 25 °C are calculated by the present dataset as Δ_fG° = -1904.077 kJ mol⁻¹ and Δ_fH° = -2038.154 kJ mol⁻¹. The corresponding values of the study by Jacob et al.^[22] are Δ_fG° = -1904.040 kJ mol⁻¹ and Δ_fH° = -2038.033 kJ mol⁻¹.

The remaining solid phase to be modeled is metallic tantalum with its oxygen solubility. The SGTE data are adopted for pure tantalum in the body-centered cubic (bcc) structure. An overview of the oxygen solubility in metallic Ta in equilibrium with Ta₂O₅ or the melt has already been compiled by Garg et al.,^[16] the most comprehensive investigation being that by Jehn and Olzi.^[17] These data on the oxygen solubility in Ta were selected for the present assessment in addition to the results by Gebhardt and Seghezzi^[21] and Fromm and Kirchheim.^[18]

After optimizing the coefficients of the Gibbs energy functions for the solid phases, the last step of the assessment followed, in which the optimization takes into account the melting equilibria. Experimental studies on the thermodynamics of Ta–O melts have not yet been performed. In the present assessment, the data for the phase diagram were taken from the work of Jehn and Olzi.^[17] However, here the melting equilibria could only be determined for the monotectic and the eutectic reactions. Their temperatures were determined by incipient melting experiments and the corresponding phase compositions were obtained by quantitative metallography of samples solidified in an arc-melter. The liquidus lines were then estimated according to the data of the invariant equilibria.

3.2. Al–Ta–O

For the ternary system, the partially ionic liquid model is used to describe the liquid state.

In the dataset for the metallic system Al–Ta, the description of the melt has to be converted from a substitutional model to the ionic liquid model.

The binary parameters for the Al–O system were accepted from Taylor et al.,^[7] because the Ta–O binary is modeled only with ions in the ionic liquid and therefore, better compatibility within the ternary liquid description is achieved in comparison with the parameters of Hallstedt.^[6] For the binary Ta–O system, the parameters of the present work are used. The Al–Ta binary parameters were accepted from the work of Witusiewicz et al.,^[14] but the original substitutional model had to be changed to the ionic liquid model. The liquid phase of the ternary system is completely modeled with an ionic liquid model containing only ions and no neutral species.

The parameters for the liquid of Witusiewicz et al. were taken as presented but described with anions instead of neutral species. No change in Gibbs energy values and therefore no change in the phase diagram calculation resulted out of this model change.

The phase model for the ternary ionic liquid is (Al³⁺, Ta²⁺, Ta⁵⁺)_P(O²⁻, Va)_Q.

King et al.^[27] published experimental data in the quasibinary section Al₂O₃–Ta₂O₅. They provided fusion temperatures for several compositions in the system. Only one ternary phase has been found which they called the Z-phase. The Z-phase in their constructed diagram can be referred to the ternary oxide AlTaO₄. They found large homogeneity ranges for the Z-phase (up to 20 mol% solubility for Al₂O₃) and Ta₂O₅ (up to 10 mol% Al₂O₃). The fusion temperatures for the samples containing 14.3 mol% up to 85.7 mol% Ta₂O₅ are measured within a range of 70 K. The main information accepted from King et al. is that only one ternary oxide AlTaO₄ exists in the quasibinary section. Homogeneity ranges and equilibria with the liquid phase must be investigated experimentally for an optimization and are therefore not implemented or modeled in this assessment.

Roth and Waring^[28] and later Schmid and Fung^[29] analyzed the tantalum pentoxide-rich side of the quasibinary section Al₂O₃–Ta₂O₅. Roth et al. found a homogeneity range of the pentoxide for high-temperature modification. For low-temperature modification, only equilibria with AlTaO₄ are detected. Schmid and Fung analyzed samples with 4–8 mol% Al₂O₃. Their X-ray analysis shows no second phase up to 7 mol% of alumina. Above that value, reflections of a second phase arise, but no more detailed information about the solubility range and the phase diagram is given. Yamaguchi et al.^[30] presented results of XRD and DTA experiments on metastable tantalum pentoxide and show that metastable solid solutions with up to 50 mol% alumina transform into the stable tantalum pentoxide and the stable aluminum tantalate AlTaO₄.

Experiments with samples in thermodynamic equilibrium have to show how a possible homogeneity range changes with composition and temperature. Because such data is not available, the phases are modeled as stoichiometric in this assessment.

An ab initio calculation for the formation energy of AlTaO₄ that results in a value of -3.412 eV is provided by Materials Project.^[31] This value refers to the formation from the pure elements. In this work, the parameters for AlTaO₄ are obtained using the Gibbs energy values of the compounds Al₂O₃ and Ta₂O₅. Therefore, the value obtained from the density functional theory (DFT) data is transferred to the enthalpy increment for the formation from the compounds Al₂O₃ and Ta₂O₅ (-19 300 J) and is then directly used as a coefficient in the parameter for the AlTaO₄ phase.

3.3. Al–Nb–O

The binary parameters for the Al–O binary were accepted from Hallstedt.^[6] For the Nb–O binary, the parameters of Massih and Jerlerud Pérez^[8] were accepted. The Al–Nb binary parameters were accepted from the work of Witusiewicz et al.,^[11] but again, the parameters of the liquid phase have to be converted to the ionic liquid model. The phase model for the ternary ionic liquid is $(\text{Al}^{3+}, \text{Nb}^{2+}, \text{Nb}^{5+})_{\text{P}}(\text{O}^{2-}, \text{Va}, \text{NbO}_2, \text{NbO}_{5/2}, \text{AlO}_{3/2})_{\text{Q}}$. As neutral species were used in the literature^[8] when modeling the oxidic melt of the binary system Nb–O, a corresponding associate ($\text{AlO}_{3/2}$) was also introduced for the present work when the model was extended to the ternary system with Al. This creates a certain incompatibility with the modeling of the melt in the Al–Ta–O system, in which only simple ions and charged vacancies were used. However, this problem has to be solved only when the datasets for Al–Nb–O and Al–Ta–O are combined, which is reserved for future work.

Zhang and Chang^[32] published an isothermal section at 1100 °C. In **Figure 1** (calculated with our dataset at 1100 °C and without ternary phases), the phase equilibria are in accordance to those shown by Zhang and Chang.^[32] The experimental focus of that work was on the niobium–alumina two-phase region Nb–Al₂O₃. No ternary compounds were considered.

Fedorov et al.^[33] investigated the quasibinary section Al₂O₃–Nb₂O₅ experimentally and a phase diagram was constructed. They found experimental evidence for the existence of three ternary oxides, namely, AlNbO₄, AlNb₁₁O₂₉, and AlNb₄₉O₁₂₄. The authors used DTA, as well as XRD, with quenched samples to verify their phase diagram with multiple sample compositions at multiple temperatures from 1400 up to 2000 °C. All three ternary phases were treated as stoichiometric compounds. A peritectic reaction at 1560 °C and two eutectic reactions at 1425 and 1435 °C are shown. The compounds AlNb₁₁O₂₉ and AlNb₄₉O₁₂₄ are analyzed to melt without decomposition in congruent melting points at 1450 and 1460 °C, respectively.

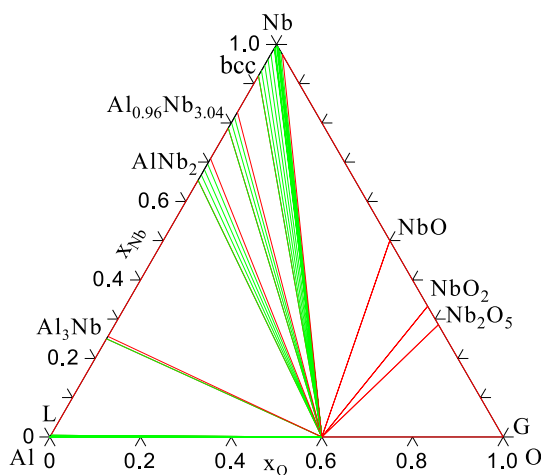


Figure 1. Isothermal section of the Al–Nb–O system at 1100 °C (this work), calculated to show the phase equilibria according to Zhang et al.^[32]

Burdese et al.^[34] also investigated this quasibinary section. They show a homogeneity range for the AlNbO₄ phase, but no other publication could confirm such a solid solution and therefore, the phase is described as stoichiometric.

An ab initio calculation for the formation energy of AlNbO₄ that results in a value of –3.236 eV is provided by Materials Project.^[35] This value refers to the formation from the pure elements. In this work, the parameters for AlNbO₄ are obtained using the Gibbs energy functions of the compounds Al₂O₃ and Nb₂O₅. Therefore, the value obtained from the DFT data is transferred to the enthalpy increment for the formation from the compounds Al₂O₃ and Nb₂O₅ (–18 622 J) and is then directly used as a coefficient in the parameter for the AlNbO₄ phase.

The remaining coefficients of the dataset are solely optimized based on phase diagram data.

4. Results and Discussion

4.1. Ta–O

In the dataset of the present assessment, the phases of the Ta–O system are described by different models. Metallic tantalum with some dissolved oxygen is represented by bcc Ta with oxygen in the interstitial sublattice and the two modifications of Ta₂O₅ are described as stoichiometric compounds. The melt is represented by the partially ionic liquid model^[3] with the species Ta²⁺ and Ta⁵⁺ in the cationic sublattice and O^{2–} and vacancies (Va) in the second sublattice. Even though only tantalum oxide with Ta⁵⁺ cations occurs in the stable phase diagram, Ta²⁺ ions were also used to model the melt, as this improved the fit of the experimental data to some extent. The lower oxidation state of tantalum is also conceivable because several metastable tantalum oxides have been described in the literature, as reviewed by Garg et al.^[16] However, according to this list of metastable oxides, additional oxidation states for tantalum are also possible. However, due to the lack of thermodynamic data for the melt, such as oxygen activities and mixing enthalpies as functions of composition and temperature, a model with more than the aforementioned ionic species seems unpromising.

The assessed thermodynamic parameters for these phases are listed in **Table 1**. All parameters are valid for the temperature range 298.15 K < T < 6000 K.

The calculated phase diagram of Ta–O is shown in **Figure 2**. For comparison, the data for the invariant equilibria recommended by Garg et al.^[16] are included. The temperatures of the invariant reactions are very well reproduced. However, the composition of the liquid in the eutectic and the composition of the Ta-rich liquid in the monotectic reaction show distinct deviations from the experimental values. The composition of the liquid in the eutectic should be 71 at% O,^[16,17] while the calculation with our dataset results to 68 at%. In the Ta-rich liquid of the monotectic, the deviation is even more pronounced. However, in the O-rich liquid of the monotectic, the calculated and the experimental values are in good agreement. In principle, by increasing the number of interaction parameters in the model of the liquid, it would be possible to improve the fit between the data and the calculation. However, a model should not contain more parameters than there is data to determine them. In view of

Table 1. CALPHAD model parameters for the Ta–O system.

Phase	Thermodynamic parameters and coefficients
Liquid	${}^0G_{\text{Ta}^{2+};\text{Va}} = \text{GLIQTAL}^{[26]}$
$(\text{Ta}^{2+}, \text{Ta}^{5+})_{\text{P}} (\text{O}^{2-}, \text{Va})_{\text{Q}}$	${}^0G_{\text{Ta}^{5+};\text{Va}} = \text{GLIQTAL} + 400000$ ${}^0G_{\text{Ta}^{2+};\text{O}^{2-}} = -2087864 + 1494.72 \cdot T - 235.136 \cdot T \cdot \ln(T)$ ${}^0G_{\text{Ta}^{2+};\text{O}^{2-}} = 0.2 \cdot {}^0G_{\text{Ta}^{5+};\text{O}^{2-}} + 0.6 \cdot \text{GLIQTAL} - 144050 - 230 \cdot T$ ${}^0L_{\text{Ta}^{2+}, \text{Ta}^{5+};\text{O}^{2-}} = 0.0$ ${}^1L_{\text{Ta}^{2+}, \text{Ta}^{5+};\text{O}^{2-}} = +155877 - 60 \cdot T$
bcc $(\text{Ta})_1(\text{O}, \text{Va})_3$	${}^0G_{\text{Ta};\text{Va}} = \text{GHSERTA}^{[26]}$ ${}^0G_{\text{Ta};\text{O}} = \text{GHSERTA} + 3 \cdot \text{GHSEROO}$ ${}^0L_{\text{Ta};\text{O}, \text{Va}} = -1130200 + 291 \cdot T$
$\alpha\text{-Ta}_2\text{O}_5$ stoichiometric	${}^0G_{\text{Ta};\text{O}} = -2095351 + 1035 \cdot T - 172.136 \cdot T \cdot \ln(T) - 0.00935 \cdot T^2$
$\beta\text{-Ta}_2\text{O}_5$ stoichiometric	${}^0G_{\text{Ta};\text{O}} = -2089535 + 833.866 \cdot T - 142.29 \cdot T \cdot \ln(T) - 0.027725 \cdot T^2 + 2.4824 \cdot 10^{-6} \cdot T^3 + 987545 \cdot T^{-1}$

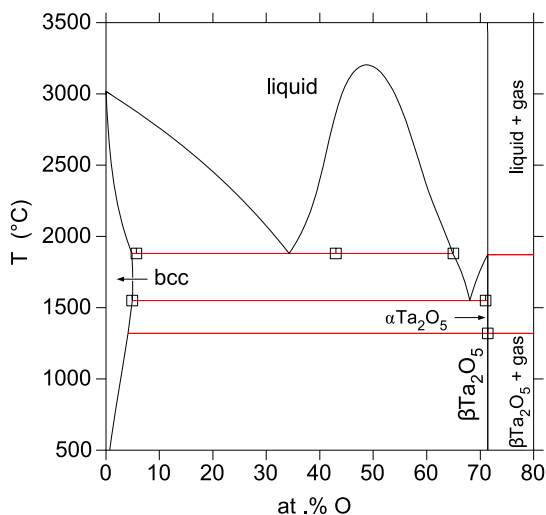


Figure 2. TaO phase diagram with transition data recommended by Garg et al.^[16]

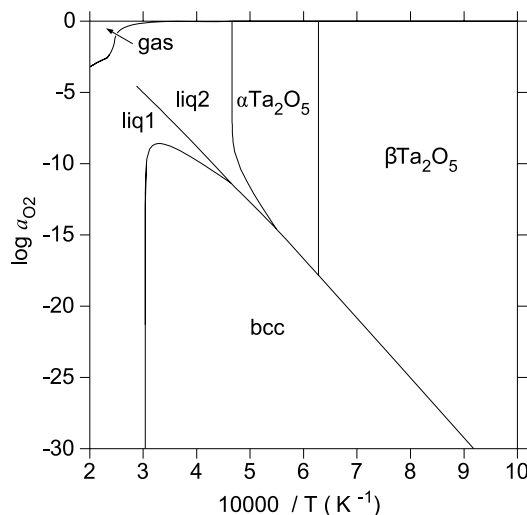


Figure 4. Ta–O stability diagram.

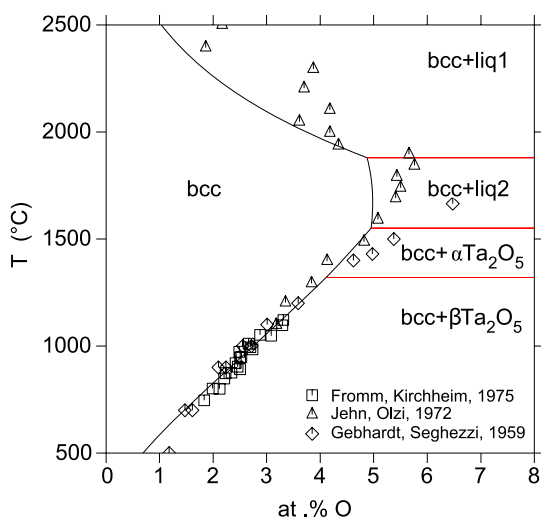


Figure 3. Oxygen solubility in metallic Ta compared with selected experimental data.^[17,18,21]

the aforementioned lack of experimental data, these deviations are tolerated in the present assessment.

Figure 3 shows an enlarged section of the calculated phase diagram, in which the solvus and solidus lines of the bcc phase are compared with the experimental oxygen solubility in tantalum by Fromm and Kirchheim,^[18] Gebhardt and Seghezzi,^[21] and Jehn and Olzi.^[17] The diagram reveals a very good agreement between the data and the calculation of equilibria between the bcc phase and the solid modifications of Ta_2O_5 . However, in the equilibria of the bcc phase with the liquid, the calculated solidus lines are clearly located at too small oxygen concentrations. The reason for this is probably related to the still unsatisfactory modeling of the melt, which is discussed in connection with **Figure 2**.

Figure 4 presents the stability ranges of the phases as a function of oxygen activity and temperature. Pure gas under normal pressure is chosen as the reference state for oxygen, so that the oxygen activities correspond to the partial pressures in bar.

During the final stage of preparing the present manuscript, another assessment of the binary system Ta–O by Meisner et al.^[15] became available where the authors provided two datasets which differ in the modeling of the melt. In one of their datasets, the liquid is described by the ionic liquid model, which is also used in the present work. In the second version, Meisner et al.^[15] use an associate model, where the liquid contains Ta_2O_5

Table 2. Comparison of the data for the monotectic and the eutectic equilibria in the Ta–O system. The compositions are given in the same sequence as the phases appear in the equilibrium equations.

Equilibrium	T [°C]	Compositions [at% oxygen]			Ref.
liquid1 ↔ bcc + liquid2 (monotectic)	1880	34.2	4.9	64.9	this work
	1880 ± 30	43.0	5.7	65.0	[16,17]
	1738	29.3	5.1	58.6	[15] ionic
	1920	27.6	5.1	58.1	[15] associate
liquid2 ↔ bcc + αTa ₂ O ₅ (eutectic)	1550	68.0	5.0	71.4	this work
	1550 ± 30	71.0	5.0	71.4	[16,17]
	1514	61.3	4.8	71.4	[15] ionic
	1641	60.3	5.5	71.4	[15] associate

species in addition to the atomic species. In the following, these two assessments are briefly compared with the present work.

In the subsolidus range, both thermodynamic descriptions of the Ta–O system by Meisner et al.^[15] are almost equivalent to the results of the present work, but in the range of equilibria involving the liquid, several differences exist. The comparison of our Figure 3 with the corresponding diagrams by Meisner et al.^[15] reveals that in their assessments the solidus lines of the bcc phase are in better agreement with the experimental data than in our work. If, on the other hand, the composition of the liquid is considered in the equilibria of the bcc phase with the melt, then the dataset of the present work shows better agreement with the experimental data. In Table 2, the data for the monotectic and the eutectic equilibria are shown and the assessed dataset is compared with experimental results. The different assessments by Meisner et al.^[15] are denoted by additional labels in the column of the references.

The table reveals that the temperatures calculated with the dataset of the present work are in excellent agreement with the experimental results for both the monotectic and the eutectic equilibria, whereas the corresponding results of both datasets of Meisner et al.^[15] are outside of the experimental uncertainty interval, as given by Jehn and Olzi.^[17]

The comparison of the phase compositions in the monotectic shows that the oxygen content of the Ta-rich melt is calculated as much too low with all datasets, although the present work comes closest to the experimental value. The experimental composition of the O-rich melt, on the other hand, agrees well with the calculation from the present work, while the results of Meisner et al.^[15] are more than 6 at% too low in both cases. In the case of the eutectic melt, the calculation with the dataset of the present work results in an oxygen content that is 3 at% too low, while the corresponding values from Meisner are about 10 at% too low.

According to the comparison of the assessments of the system Ta–O, the dataset of the present work seems preferable although it still contains the depicted limitations for the liquid phase.

4.2. Al–Ta–O

The binary thermodynamic parameters and coefficients for the Al–Ta–O system are taken from the literature and the ternary oxide is added. As described at the end of Section 3.2, the

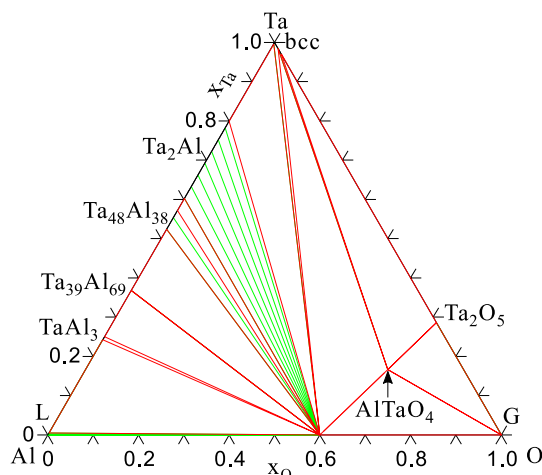


Figure 5. Isothermal section of the Al–Ta–O system at 1100 °C with ternary oxide (this work).

temperature-independent coefficient of the AlTaO₄ parameters is set to the calculated formation energy from Materials Project.^[31] The second coefficient is used to stabilize the phase from room temperature to its melting point of 1693 °C, which is in very good agreement with the experimental results of King et al.^[27] As no other reliable data for solid–liquid equilibria in this system is available, no parameters for the liquid phase are assessed. Only the extrapolation of the binary parameters is used.

A two-phase region (Ta)–Al₂O₃ is calculated to be stable up to the melting temperature of alumina and shows the thermodynamic stability of a composite consisting of those two materials. Figure 5 shows the isothermal section at 1100 °C, in which the two-phase field region can be seen.

A three-phase region (Ta)–Al₂O₃–AlTaO₄ is also calculated. An oxygen impurity in a tantalum–alumina composite will lead to the formation of AlTaO₄ if the oxygen impurity concentration is higher than the limit that the metal solid solution can dissolve.

The entropy at constant volume of AlTaO₄ is available in an online database for ab initio phonon calculations^[36] and is 95.4 J K^{−1} mol^{−1} at 25 °C. The entropy at constant pressure calculated from our dataset is 95.0 J K^{−1} mol^{−1} at 25 °C. A comparison for higher temperatures is not applied because the deviation between the entropy at constant volume and the entropy at constant pressure will increase over temperature. The ab initio calculation for constant volume is used to validate the assessed parameters to some extent but is not directly used in the optimization.

The assessed ternary parameters are listed in Table 3. The ternary parameters in both systems are valid from 298.15 up to 6000 K. As described, the parameters were assessed using the phase diagram data of King et al.^[27] and Fedorov et al.,^[33] as well as DFT data.^[31,35]

4.3. Al–Nb–O

In the ternary system Al–Nb–O, a two-phase region (Nb)–Al₂O₃ is also calculated and shows the thermodynamic compatibility of

Table 3. Thermodynamic parameters for the ternary systems Al–M–O (M = Nb, Ta).

System	Phase	Thermodynamic parameters and coefficients
Al–Nb–O	Liquid	${}^0L_{\text{AlO}_{3/2}, \text{NbO}_{5/2}} = +121310 - 65.986 \cdot T$
		${}^1L_{\text{AlO}_{3/2}, \text{NbO}_{5/2}} = +6707.4 + 12.682 \cdot T$
		${}^0L_{\text{Nb}^{2+}; \text{AlO}_{3/2}, \text{Va}} = +50000$
		${}^0G_{\text{AlNbO}_4} = 0.5 \cdot G_{\text{Al}_2\text{O}_3} + 0.5 \cdot G_{\text{Nb}_2\text{O}_5} - 18622 + 4.1500 \cdot T$
Al–Nb–O	Liquid	${}^0G_{\text{AlNb}_{11}\text{O}_{29}} = 0.5 \cdot G_{\text{Al}_2\text{O}_3} + 5.5 \cdot G_{\text{Nb}_2\text{O}_5} - 212170 + 109.22 \cdot T$
		${}^0G_{\text{AlNb}_{49}\text{O}_{124}} = 0.5 \cdot G_{\text{Al}_2\text{O}_3} + 24.5 \cdot G_{\text{Nb}_2\text{O}_5} - 153730 + 110.38 \cdot T$
Al–Ta–O	AlTaO ₄	${}^0G_{\text{AlTaO}_4} = 0.5 \cdot G_{\text{Al}_2\text{O}_3} + 0.5 \cdot G_{\text{Ta}_2\text{O}_5} - 19300 + 3.49 \cdot T$

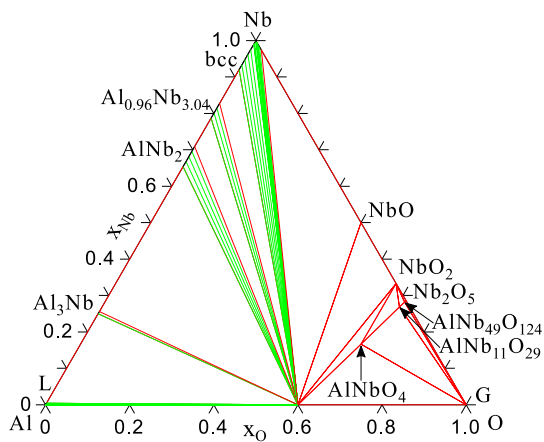


Figure 6. Isothermal section of Al–Nb–O at 1100 °C with ternary oxides (this work).

this material combination. In contrast to the tantalum system, no ternary oxide participates in the neighboring three-phase region (Figure 6). Instead, niobium, alumina, and niobium monoxide are in equilibrium in that region. An oxygen impurity concentration higher than the solubility limit in the metal solid solution will allow the niobium monoxide to form.

For the quasibinary section (Figure 7), parameters for the ternary oxides and liquid are optimized to fit the experimental data of Fedorov et al.^[33] The calculated peritectic decomposition of AlNbO₄ is in good agreement with the experimental data. A small deviation to the interpolated curve drawn by Fedorov et al.^[33] can be detected in the high-temperature alumina-liquid equilibria. This deviation is a consequence of the chosen parameter set to model the low-temperature solid–liquid equilibria according to the experimental data. The resulting metastable miscibility gap in the liquid is shown with dashed lines in Figure 7. The melting points of the other two ternary oxides agree well with the experimental data.

The temperatures of the invariant reactions are listed in Table 4. The only major deviation from the phase diagram of Fedorov et al.^[33] is the composition of the liquid in the eutectic liquid à AlNbO₄ + AlNb₁₁O₂₉. Fedorov et al.^[33] provide no experimental data for this composition and it is mentioned solely in

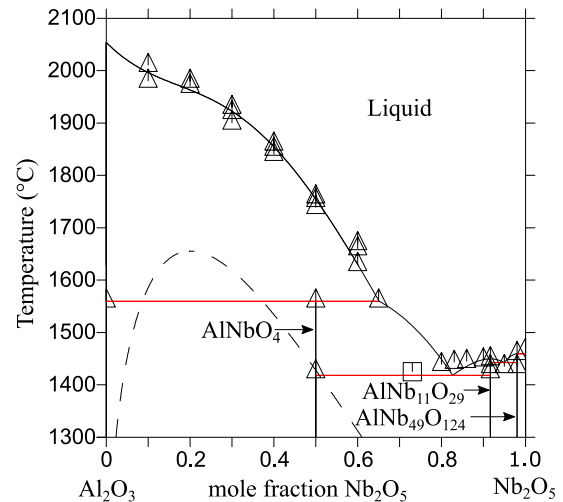


Figure 7. Calculated quasibinary section Al₂O₃–Nb₂O₅ (this work). Δ: experimental data points,^[33] □: phase diagram point,^[33] dashed line: metastable miscibility gap in the ionic liquid.

Table 4. Temperatures of invariant and congruent transitions.

Transitions	This work	Fedorov et al. ^[33]
Liquid + Al ₂ O ₃ → AlNbO ₄	1560 °C	1560 ± 10 °C
Liquid → AlNbO ₄ + AlNb ₁₁ O ₂₉	1418 °C	1425 ± 10 °C
Liquid → AlNb ₁₁ O ₂₉ + AlNb ₄₉ O ₁₂₄	1443 °C	1435 ± 10 °C
AlNb ₁₁ O ₂₉ , congruent melting point	1450 °C	1450 ± 10 °C
AlNb ₄₉ O ₁₂₄ , congruent melting point	1460 °C	1460 ± 10 °C

the conclusion of their work. The stated value of 73 mol% Nb₂O₅ is marked with a different symbol in Figure 7 to indicate the missing experimental confirmation. As no experimental data for the hypoeutectic solid–liquid equilibria is given in the study by Fedorov et al.^[33] and the deviation in our calculations is accepted. The eutectic must be experimentally investigated in a future work.

The entropy at constant volume of AlNbO₄ is available in an online database for ab initio phonon calculations^[36] and is 93.0 J K^{−1} mol^{−1} at 25 °C. The entropy at constant pressure (calculated, this work) is 90.0 J K^{−1} mol^{−1} at 25 °C. A comparison for higher temperatures is not applied because the deviation between the entropy at constant volume versus the entropy at constant pressure will increase over temperature. The ab initio calculation for constant volume is used to validate the assessed parameters to some extent but is not directly used in the optimization.

The data of Table 3 reveal that the entropy of formation related to 1 mol of metal atoms is 2.1 J K^{−1} mol^{−1} for AlNbO₄, 9.1 J K^{−1} mol^{−1} for AlNb₁₁O₂₉, and 2.2 J K^{−1} mol^{−1} for AlNb₄₉O₁₂₄. The high value for AlNb₁₁O₂₉ is caused by adjusting the parameters to the eutectic temperature of the reaction liquid à AlNbO₄ + AlNb₁₁O₂₉. The enthalpy and entropy parameters of the ternary oxides AlNb₁₁O₂₉ and AlNb₄₉O₁₂₄ are solely based on the optimization using phase diagram data. However, as

mentioned in Section 1, calorimetric experiments on the aluminum niobates are planned for the near future, and a more detailed discussion of the formation data has to be postponed until the corresponding results are available.

5. Conclusion

A thermodynamic dataset for the Ta–O system is assessed which allows for the calculation of the phase diagram and thermochemical data of the system. In the subsolidus range, the calculations are in good agreement with the experimental data, whereas in equilibria involving the liquid, certain deviations to the literature data remain. Thermodynamic datasets for the ternary systems Al–Nb–O and Al–Ta–O are obtained by assessments based on literature data and the presented binary parameters. The datasets allow the calculation of phase equilibria for the synthesis and long-term usage of refractory metal ceramic composites. The dataset for the Al–Nb–O system contains three ternary aluminum niobates which are located in the quasibinary section $\text{Al}_2\text{O}_3\text{–Nb}_2\text{O}_5$. This quasibinary section is calculated in agreement with the literature. The dataset for Al–Ta–O includes AlTaO_4 , which is the only stable ternary oxide of this system. As the experimental data on this oxide are very scarce, the assessment of Al–Ta–O is only preliminary. Therefore, further experimental work on this system is under preparation.

Acknowledgements

The authors gratefully acknowledge funding by the German Research Foundation (DFG) within the Research Unit FOR3010 (project number: 416817512), reference numbers FR1108/3-1 and SE647/23-1.

Open Access funding enabled and organized by Projekt DEAL.

Conflict of Interest

The authors declare no conflict of interest.

Data Availability Statement

The data that support the findings of this study are available in the supplementary material of this article.

Keywords

aluminum niobates, aluminum tantalates, CALculation of PHase Diagrams, thermodynamics

Received: January 31, 2022

Revised: May 16, 2022

Published online:

[1] G. Cacciamani, *Technol. Met. Mater. Min.* **2016**, 13, 16.

[2] H. Lukas, S. G. Fries, B. Sundman, *Computational Thermodynamics: The Calphad Method*, Cambridge University Press, Cambridge **2007**.

- [3] M. Hillert, B. Jansson, B. Sundman, J. Ågren, *Metall. Trans. A* **1985**, 16, 261.
- [4] N. Saunders, A. P. Miodownik, *CALPHAD (Calculation of Phase Diagrams): A Comprehensive Guide*, Elsevier, Amsterdam **1998**.
- [5] J. O. Andersson, T. Helander, L. Höglund, P. F. Shi, B. Sundman, *Calphad* **2002**, 26, 273.
- [6] B. Hallstedt, *J. Phase Equilib.* **1993**, 14, 662.
- [7] J. R. Taylor, A. T. Dinsdale, M. Hillert, M. Selleby, *Calphad* **1992**, 16, 173.
- [8] A. R. Massih, R. Jerlerud Pérez, Thermodynamic Evaluation of the Nb–O System, Quantum Technologies AB, Stockholm PM **2006**, Vol. 05, p. v2.
- [9] N. Dupin, I. Ansara, System Nb–O. Unpublished communication to the authors of reference [8].
- [10] Z. Zhu, Y. Du, L. Zhang, H. Chen, H. Xu, C. Tang, *J. Alloys Compd.* **2008**, 460, 632.
- [11] V. T. Witusiewicz, A. A. Bondar, U. Hecht, T. Velikanova, *J. Alloys Compd.* **2009**, 472, 133.
- [12] C. He, F. Stein, M. Palm, *J. Alloys Compd.* **2015**, 637, 361.
- [13] Y. Du, R. Schmid-Fetzer, *J. Phase Equilib.* **1996**, 17, 311.
- [14] V. T. Witusiewicz, A. A. Bondar, U. Hecht, J. Zollinger, V. M. Petyukh, O. S. Fornichov, V. M. Voblikov, S. Rex, *Intermetallics* **2010**, 18, 92.
- [15] K. J. Meisner, R. Zaman, B.-C. Zhou, *Calphad* **2022**, 76, 102391.
- [16] S. P. Garg, N. Krishnamurthy, A. Awasthi, M. Venkatraman, *J. Phase Equilib.* **1996**, 17, 63.
- [17] H. Jehn, E. Olzi, *J. Less-Common Met.* **1972**, 27, 297.
- [18] E. Fromm, R. Kirchheim, *Z. Metallk.* **1975**, 66, 144.
- [19] W. Nickerson, C. Altstetter, *Scr. Metall.* **1973**, 7, 377.
- [20] J. S. Lee, C. J. Altstetter, *Acta Metall.* **1986**, 34, 139.
- [21] E. Gebhardt, H. Seghezzi, *Z. Metallk.* **1959**, 50, 521.
- [22] K. T. Jacob, C. Shekhar, Y. Waseda, *J. Chem. Thermodyn.* **2009**, 41, 748.
- [23] S. Ignatowicz, M. W. Davies, *J. Less-Common Met.* **1968**, 15, 100.
- [24] T. Rezukhina, L. Kravchenko, *J. Chem. Thermodyn.* **1972**, 4, 655.
- [25] M. W. Chase, C. A. Davis, J. R. Downey, D. J. Frurip, R. A. McDonald, A. N. Syverud, *J. Phys. Chem. Ref. Data* **1985**, 14, 1715.
- [26] A. T. Dinsdale, *Calphad* **1991**, 15, 317.
- [27] B. W. King, J. Schultz, E. A. Durbin, W. H. Duckworth, *Some Properties of Tantalum Systems*, Battelle Memorial Inst., Columbus, **1956**.
- [28] R. S. Roth, J. L. Waring, *J. Res. Natl. Bur. Stand., Sect. A* **1970**, 74A, 485.
- [29] S. Schmid, V. Fung, *Aust. J. Chem.* **2012**, 65, 851.
- [30] O. Yamaguchi, D. Tomihisa, T. Uegaki, K. Shimizu, *J. Am. Ceram. Soc.* **1987**, 70, C-335.
- [31] K. Persson, Materials Data on TaAlO₄ (SG:12) by Materials Project, **2014**, <https://doi.org/10.17188/1190615>.
- [32] M. X. Zhang, Y. A. Chang, *J. Phase Equilib.* **1994**, 15, 470.
- [33] N. F. Fedorov, I. F. Andreev, R. M. Kasparyan, T. P. Smorodina, *Izv. Akad. Nauk SSSR, Neorg. Mater.* **1971**, 7, 643.
- [34] A. Burdese, M. Lucco-Borlera, P. Rolando, *Atti Accad. Sci. Torino, Cl. Sci. Fis., Mat. Nat.* **1964-1965**, 99, 1079ff.
- [35] K. Persson, Materials Data on NbAlO₄ (SG:12) by Materials Project, **2014**, <https://doi.org/10.17188/1202082>.
- [36] Online database of phonon computations, <http://phonondb.mtl.kyoto-u.ac.jp/>.